Microclimate temperature variations from boreal forests to the tundra

Aalto, Juha

2022-08-15

Aalto , J , Tyystjärvi , V , Niittynen , P O , Kemppinen , J , Rissanen , T K , Gregow , H & Luoto , M 2022 , ' Microclimate temperature variations from boreal forests to the tundra ' , Agricultural and Forest Meteorology , vol. 323 , 109037 . https://doi.org/10.1016/j.agrformet.2022.109037

http://hdl.handle.net/10138/346136
https://doi.org/10.1016/j.agrformet.2022.109037

Agricultural and Forest Meteorology 323 (2022) 109037

Contents lists available at ScienceDirect

Agricultural and Forest Meteorology

journal homepage: www.elsevier.com/locate/agrformet

Microclimate temperature variations from boreal forests to the tundra

Juha Aalto [a,b,*], Vilna Tyystjärvi [a,b], Pekka Niittynen [b], Julia Kemppinen [c], Tuuli Rissanen [b], Hilppa Gregow [a], Miska Luoto [b]

[a] Finnish Meteorological Institute, P.O. Box 503, Helsinki FI-00101, Finland
[b] Department of Geosciences and Geography, University of Helsinki, P.O. Box 64, Gustaf Hällströmin katu 2a, Helsinki FI-00014, Finland
[c] The Geography Research Unit, University of Oulu, P.O. Box 8000, Oulu FI-90014, Finland

ARTICLE INFO

Keywords:
Surface temperature
Soil temperature
Air temperature
Wetlands
Thermal heterogeneity

ABSTRACT

Microclimate varies greatly over short horizontal and vertical distances, and timescales. This multi-level heterogeneity influences terrestrial biodiversity and ecosystem functions by determining the ambient environment where organisms live in. Fine-scale heterogeneity in microclimate temperatures is driven by local topography, land and water cover, snow, and soil characteristics. However, their relative influence over boreal and tundra biomes and in different seasons, has not been comprehensively quantified. Here, we aim to (1) quantify temperature variations measured at three heights: soil (-6 cm), near-surface (15 cm) and air (150 cm), and (2) determine the relative influence of the environmental variables in driving thermal variability. We measured temperature at 446 sites within seven focus areas covering large macroclimatic, topographic, and ecosystem gradients (tundra, mires, forests) of northern Europe. Our data, consisting of over 60 million temperature readings during the study period of 2019/11–2020/10, reveal substantial thermal variability within and across the focus areas. Near-surface temperatures in the tundra showed the greatest instantaneous differences within a given focus area (32.3 °C) while the corresponding differences for soil temperatures ranged from 10.0 °C (middle boreal forest) to 27.1 °C (tundra). Instantaneous differences in wintertime air temperatures were the largest in the tundra (up to 25.6°C, median 4.2 °C), while in summer the differences were largest in the southern boreal forest (13.1°C, median 4.8°C). Statistical analyses indicate that monthly-aggregated temperature variations in boreal forests are closely linked to water bodies, wetlands, and canopy cover, whereas in the tundra, variation was linked to elevation, topographic solar radiation, and snow cover. The results provide new understanding on the magnitude of microclimate temperature variability and its seasonal drivers and will help to project local impacts of climate change on boreal forest and tundra ecosystems.

1. Introduction

Boreal forest and tundra biomes cover one third of Earth's terrestrial surface and are experiencing rapid climatic warming with severe consequences (Post et al. 2009). These high-latitude biomes also play a key role in the global climate system, storing an estimated 50% of global soil carbon (McGuire et al., 2009; Virkkala et al., 2021). The warming trend is projected to continue during the upcoming decades with the most pronounced changes projected to occur during the winter season (Ruosteenoja et al. 2016, 2019; Bintanja and Andry, 2017). To track these changes and their impacts, climate change research heavily relies on coarse-gridded macroclimate data (Flato, 2011; Bedia et al., 2013; Lenoir et al., 2013; Gardner et al., 2019). However, local climate conditions can differ substantially from those represented by these macroclimatic temperature grids (e.g., Lembrechts et al., 2019; Haesen et al., 2021). Thus, recently there has been a renewed focus on microclimate owing to its paramount importance in understanding how organisms and ecosystems respond to climate change (Potter et al., 2013; De Frenne et al., 2021).

The impact of macroclimate on ecosystems is filtered through physiographic, edaphic, and biotic characteristics of the landscape (Ashcroft and Gollan, 2013; Lenoir et al., 2017). These microclimatic drivers alter air mixing, heat transfer and budgets of short- and long-wave radiation, that potentially lead to contrasting wind, thermal, and humidity conditions within short horizontal and vertical distances (Barry and Blanken, 2016). Further, these conditions create microclimates where local temperatures can considerably differ from the macroclimate (Dobrowski, 2011; Graae et al., 2012; De Frenne et al., 2019).

* Corresponding author at: Finnish Meteorological Institute, P.O. Box 503, Helsinki FI-00101, Finland.
E-mail address: juha.aalto@fmi.fi (J. Aalto).

https://doi.org/10.1016/j.agrformet.2022.109037
Received 14 February 2022; Received in revised form 30 May 2022; Accepted 1 June 2022
Available online 6 June 2022

In terrestrial biomes, microclimate influences species distributions, biodiversity, and ecosystem functions by determining ambient temperatures for near-surface and soil organisms, and consequently, further influences productivity, decomposition, and carbon cycling (Greiser et al., 2018; Lembrechts et al., 2019; Niittynen et al., 2020; Zellweger et al., 2020; Seibold et at., 2021). Thus, understanding the magnitude of thermal differences in a landscape at a given time (i.e., thermal heterogeneity; Scherrer and Körner, 2011; Lenoir et al., 2013), and the relative contributions of static landscape factors (e.g., topography) and dynamic factors (e.g., canopy closure and snow cover) driving thermal heterogeneity is needed for projecting how climate change shapes ecosystems.

In boreal forests, canopy intercepts radiation (both incoming and outgoing), decelerates air flow, and affects evapotranspiration, thus creates microclimates where temperature variation is buffered compared to macroclimatic temperatures outside the canopy (Barry and Blanken, 2016; De Frenne et al., 2021). In contrast, microclimatic temperature variability may be accentuated compared to macroclimate in areas that are exposed to high radiation, sheltered from winds, and have dry soils. Vegetation drives microclimatic temperature variability also in the tundra (Aalto et al. 2013; Kemppinen et al. 2021). There, the role of local topography is expected to be especially strong due to its influence on fine-scale variation in snow accumulation, surface water flow, net radiation, and cold-air pooling under stable atmospheric conditions (Pepin et al., 2009; Daly et al., 2010; Aalto et al., 2017a; Niittynen et al., 2020). Local hydrology also influences microclimate temperatures due to the high specific heat capacity of water. This can lead to buffered temperatures in areas with high soil moisture and in areas near wetlands and water bodies (Yang et al., 2012; Ashcroft and Gollan, 2013; Słowińska et al. 2022.).

In addition to various environmental drivers, microclimate temperature also depends on the height from the surface (Barry and Blanken, 2016). In general, temperature variations are largest close to the surface, and decrease with height due to increased air mixing. Below ground, temperature variability is buffered compared to above soil surface temperatures and is controlled by soil heat flux. This, in turn, is driven by surface radiation balance, specific heat capacity of the soil (dependent on e.g., soil moisture), and seasonal snow cover that effectively insulates the ground from temperature fluctuations in the free air (Grundstein et al., 2005; Aalto et al., 2018; Fernández-Pascual and Correia-Álvarez, 2021). These vertical variations in microclimate temperatures are also relevant for different ecosystem functions. For example, soil temperatures are closely linked to e.g., soil respiration and nutrient cycling via controlling microbial activity and mycorrhiza associations (Soudzilovskaia et al., 2015; Du et al., 2020). In turn, air temperatures close to the surface are especially relevant for animals living on the surface or in the litter, plant ecophysiology and metabolism, and decomposition (Körner and Hiltbrunner, 2018; Seibold et al., 2021). Air temperature measured 1–2 m above the soil surface represents conditions relevant for larger organisms and ecosystem-level processes, such as local productivity patterns (Potter et al., 2013). However, standardized weather stations and gridded climate datasets (e.g., Fick and Hijmans, 2017; Karger et al., 2017) often ignore the vertical temperature gradients and consequently misrepresent local climate conditions relevant for many organisms and ecosystem processes (Suggitt et al., 2011; Graae et al., 2012; De Frenne and Verheyen, 2016).

The relative importance of microclimate temperature drivers can substantially differ across and within biomes (Barry and Blanken, 2016). However, in the past, most empirical microclimate studies have been conducted over single study settings with limited spatial extents (e.g., Pepin et al., 2009; Yang et al., 2012). Therefore, the understanding of the thermal characteristics across biomes and their contributing factors has remained limited. Here, we investigate microclimate temperature variation at various heights using a dense network of microclimate stations over a large geographical extent. More precisely, we aim to (1) quantify the temperature variability measured at three heights: soil (-6 cm), near-surface (15 cm) and air (150 cm), and (2) examine the relative influence of the environmental variables driving spatio-temporal variation of the temperature parameters. The study is based on a large network of miniature and low-cost microclimate stations installed at study sites (n = 446) within seven focus landscapes (hereafter focus areas) located in northern Europe. The study domain covers large gradients of macroclimate and elevation, and distinct ecosystems from both the boreal forest and tundra biomes.

2. Material and methods

2.1. Study domain and design

The study domain extends across seven focus areas in Finland from hemiboreal forests to the oroarctic tundra and covers large gradients in macroclimate, elevation, and ecosystems (Fig. 1). Climate in Finland is highly influenced by the Polar Front as well as the North Atlantic Current which drive macroclimatic temperature and precipitation patterns. These are also influenced by the Scandes mountains in the west and the landmass of the Eurasian continent in the east (Tikkanen, 2005). Along the latitudinal gradient of ca. 60–69 N, mean annual air temperatures range from -2.2°C to 7.1°C (1991–2020 period, Jokinen et al., 2021). The elevational gradient of the study domain ranges from ca. 30 to 950 meters above sea level with pronounced local and regional topographical variation due to multiple past glaciations. Moreover, due to the glaciations and the relatively humid climate, lakes and mires are abundant in Finland (Tikkanen, 2005). In the northernmost parts of the study domain, near-surface permafrost is present in peatlands outside the focus areas (Aalto et al., 2017b).

The selected focus areas are mainly situated in protected areas to minimize the influence of anthropogenic disturbance. Each focus area has 50–100 microclimate stations at which loggers were installed to measure soil and air temperature (see Table 1; Fig S1 and Section 2.3. for more details). The northernmost focus areas are in Kilpisjärvi, northwestern Finland, around Mount Malla and the Malla nature reserve (hereafter, MAL) and Mount Ailakkavaara (AIL). Another focus area in northern Finland is located in the Värriö nature reserve (VAR) in Salla and Savukoski, in the north-east. All the three northernmost areas have measurement sites above and below the forest line, and they are characterized by the boreal forest - tundra ecotone differentiating them from the central and southern areas. In central Finland, two focus areas are located within and around the Pisa nature reserve (PIS) in Kuopio and within the Tiilikkajärvi national park (TII) in Rautavaara. PIS is characterized by boreal forests and varying topography whereas TII comprises mainly mires. Another focus area characterized by mires is the Hyytiälä region (HYY) in southern Finland, where the stations are located within and nearby the Siikaneva nature reserve. The southernmost focus area is located within the Karkali nature reserve (KAR) and other nearby protected areas in Lohja, in the hemiboreal zone.

To determine the measurement sites, we conducted a random stratification to pre-select a suite of candidate locations that maximally cover the main environmental gradients within the focus areas (Fig. S2). This was done separately for each focus area. The stratification was based on several variables e.g., total canopy cover, deciduous canopy cover, distance to forest edge, elevation, potential annual incoming solar radiation, and a topographic wetness index (the SAGA wetness index), although the final selection of the variables varied depending on the distinct features of each area. First, we masked the areas outside the nature reservations and extracted the remaining pixel information on a systematic grid with a 10 m cell size. Next, we randomly selected 50% of the points and used this subset to reduce the multidimensional environmental space into its first three principal components. Then we took a sub-sample of 100 points that maximally and systematically covered the shrunk environmental space. We repeated these procedures 100 times and used the selection frequency for each point as a weight in the final random point selection. This two-step selection process was also

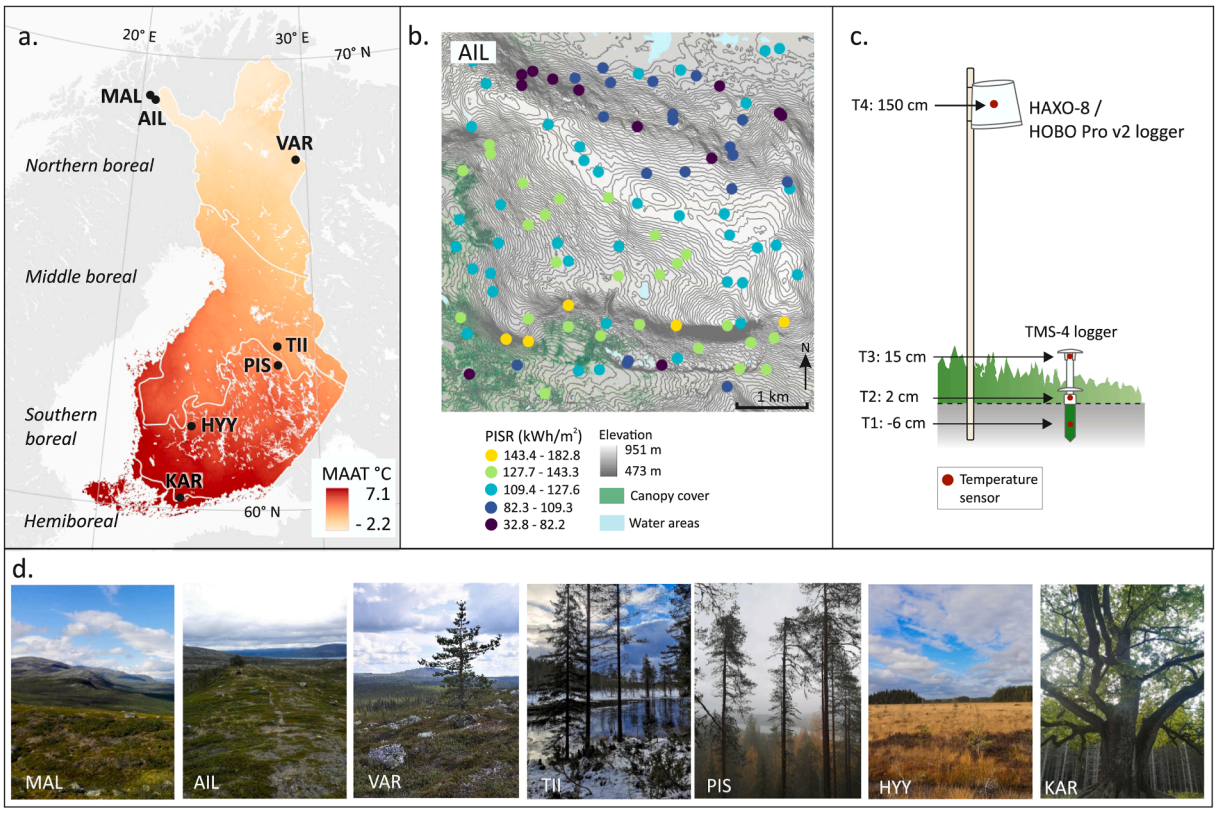

Fig. 1. Study domain and design. Panel **a** represents the locations of the seven focus areas in relation to the mean annual air temperature in Finland (MAAT; 1991–2020). The white borders mark boreal vegetation zones (in italics). White polygons represent water bodies over 10 km^2. Northernmost focus areas (MAL, AIL, VAR) are in the boreal forest–tundra ecotone comprising both northern boreal forests and oroarctic tundra. Panel **b** represents an example of the sampling design in AIL with the colored points depicting annual potential incoming solar radiation (PISR) calculated from a digital elevation model. Panel **c** depicts the logger placement and measurement heights (T1=soil, T2=surface, T3=near-surface, T4=air) at the microclimate stations. T2 was only used to derive snow cover information (see Material and methods for details). Field photos from each focus area are presented in panel **d**. Focus area abbreviations are defined in the main text and in Table 1.

Table 1
Description of the seven focus areas. Mean annual air temperature data for 1991–2020 are from Jokinen et al. (2021), and automated weather station data (AWS; Table S1) were acquired for each focus area for the period of the microclimate measurements (2019/11/01-2020/10/31).

	Focus area			Measurement setting				Mean air temperature (°C)	
	Name	Center coordinate	Sites (n)	Logger	Area (km^2)	Elevation (m)	Ecosystem	Annual 1991-2020	2019/11/01–2020/10/31
Northern Finland	**MAL:** Mount Malla, Malla nature reserve	69.071 N, 20.698 E	100	TMS-4 HOBO	23.8	482–934	Northern boreal forest - Tundra	-1.4	-0.7
	AIL: Mount Ailakkavaara	68.991 N, 21.015 E	100	TMS-4 HOBO	24.0	509–933	Northern boreal forest - Tundra	-1.4	-0.7
	VAR: Värriö nature reserve	67.736 N, 29.596 E	50	TMS-4 HAXO-8	22.7	262–475	Northern boreal forest - Tundra	0.1	1.1
Central Finland	**TII:** Tiilikkajärvi national park	63.646 N, 28.312 E	50	TMS-4 HAXO-8	17.7	187–205	Middle boreal forest	2.9	4.7
	PIS: Pisa nature reserve	63.218 N, 28.328 E	50	TMS-4 HAXO-8	16.0	103–262	Southern boreal forest	2.6	4.4
Southern Finland	**HYY**: Hyytiälä, Siikaneva nature reserve and nearby areas	61.831 N, 24.196 E	50	TMS-4 HAXO-8	51.5	152–203	Southern boreal forest	4.1	5.9
	KAR: Karkali nature reserve and surrounding protected areas	60.248 N, 23.830 E	50	TMS-4 HAXO-8	47.5	32-99	Hemiboreal forest	6.0	7.9

necessary to be able to ascertain a minimum distance (100 m) between the selected points to avoid pseudoreplication. These steps used the eSample function from iSDM R package (Hattab and Lenoir 2017). Using such a protocol, we were able to detect (and select) the points that are unique in terms of their environmental conditions and thus likely valuable locations in the station network. Selected points were visually inspected by examining the environmental variables' distributions. Final judgment of each preselected location was confirmed at the field.

2.2. Weather station data

Hourly weather station data for the study period of 2019/11/01–2020/10/31 and long-term averaged climate data for the years 1991–2020, was acquired from each focus area's nearest automated weather station (AWS) operated by the Finnish Meteorological Institute (Fig. S3; Table S1). The data have undergone an operational quality control.

2.3. Microclimate temperature data

All microclimate stations were equipped with a Tomst TMS-4 logger (Wild et al., 2019) and either a LogTag HAXO-8 (LogTag North America Inc.) or Onset HOBO U23 Pro v2 logger (Onset Computer Corporation; with exceptions of Ailakkavaara and Malla study areas which both have 100 TMS-4 loggers and 40 HAXO/HOBO loggers). The TMS-4 temperature sensors measure temperature at three heights (Fig. 1c): -6 cm for soil temperature (T1), 2 cm for surface temperature (T2), and 15 cm for near-surface temperature (T3) with a precision of 0.0625 °C and an accuracy of ± 0.5 °C. Noteworthy, in this study, T2 is used only for interpreting snow cover duration from the surface temperature values. Additionally, TMS-4 also measures soil moisture, which is used in this study as a predictor of microclimate temperature variation (see Sections 2.5. and 2.7.). We measured air temperature at 150 cm (T4) by using HAXO-8 (precision of 0.1°C; accuracy ±0.3°C for ambient temperatures of 0°C-50°C and ±0.6°C for ambient temperatures below 0°C) and HOBO loggers (precision 0.04°C; accuracy ±0.2°C from 0 to 70°C and ±0.25 from -40 to 0°C). These sensors were installed under white well-ventilated plastic radiation shields on the north side of either tree trunks or wooden poles to reduce exposure to direct solar radiation. Both sensors also measure air humidity, which was used only as a part of the data quality control in this study (see Section 2.4.). TMS-4 loggers were set to log at 15 min, HOBO loggers at 30-minute, and HAXO loggers at 2 h intervals due to different memory capacities of the loggers. To keep the 150 cm air temperature measurements comparable between the two logger types, we thinned the HOBO time series to the matching 2-h intervals of the HAXO loggers. The stations were installed in June-October 2019. The study period is one year from 2019/11/01 to 2020/10/31 which is fully covered in all the study areas.

2.4. Data preprocessing and quality control

All temperature time series were visually quality checked. If, for instance, a logger had fallen down or its radiation shield was detached, such time periods were identified, and the jeopardized measurements were removed. Additionally, four sources of error were detected and corrected: 1) sensors systematically recording too low or high temperatures, 2) erroneous peaks over one or few consecutive measurements, 3) HAXO and HOBO loggers skipping measurements but continuing to count the time after the gap from the last timestamp before the failure, thus disengaging the correct time and temperature, and 4) snow reaching the height of the HAXO and HOBO loggers (T4, 150 cm). We created the following automated procedures to correct these issues. The R code used for these steps can be found in the public focus area -specific Github repositories under user *Poniitty* (e.g., the raw data and processing code for VAR in https://github.com/poniitty/varrio_microclimate).

(1) For each sensor of the TMS-4 logger, we calculated the mean temperature over the periods when the logger was stored in its original package under stable office conditions (no signs of considerable temporal variation in temperature record) and compared these means across the three sensors within each logger. We arranged the sensors based on these means and corrected the sensors recording the highest and lowest mean temperatures to match with the middle one. Then, we used these correction temperatures to correct for systematic deviations over the whole sensor-specific time series. These corrections were mostly very minor (<0.1°C) but in some rare cases even as high as 0.5 °C. Thus, the corrections were considered to greatly improve the reliability of the dataset.
(2) To automatically detect erroneous peaks in the TMS-4 data, we iterated over all individual time series month by month and detected the logger within the same study area that best matched with the temporal pattern of the focal sensor (in terms of highest pairwise correlation and lowest root mean-squared error, RMSE). We then calculated moving averages and identified moments when the successive measurements showed a large rise or drop and when the two loggers showed suspicious differences based on the calculated statistics. By careful inspection, we set multiple criteria and thresholds for the differences to judge whether the peak in temperatures was a result of a natural event or an error. For example, an event was assessed unnatural or occur due to measurement error if two adjacent measurements (in 15-minute intervals) differed by more than 20°C or if soil temperature was suddenly increased or decreased by more than 3°C but returned right after the single-measurement peak back to the previous temperature. Erroneous peaks and their adjacent measurements were removed and replaced by linear interpolation while taking the measurements of the matching sensor into account as well.
(3) To correct for non-matching timestamps in the HOBO and HAXO data (T4), we calculated a median time series over all other loggers within each study area to which the individual logger time series were compared to. We calculated running correlations and identified breakpoints when the reference time series and a focal logger time series started to deviate from each other. If a breakpoint was identified, we started to gradually shift the temperature measurements of the focal logger and moved the post-breaking point data to a period where it reached maximum correlation with the reference period. We repeated this procedure multiple times to find all potential breaking points and to trim the gap margins efficiently. The outcomes were visually inspected to see if further corrections were needed (see an example of a corrected time series in Fig. S4).
(4) We identified periods when the HAXO/HOBO loggers were under snow by calculating variability and extremes of temperature and relative humidity from individual time series with a 5-days moving window. We selected multiple criteria (e.g., low temporal variability, maximum temperatures <0.5°C) to find the potential periods of snow coverage and if these conditions persisted for several consecutive days the measurements were removed from the dataset. After quality checks temperature data from 446 study sites was used in the analyses but the number varies by month and measuring height (see details in Fig. S5).

The deployed radiation shielding has an effect on the temperature readings as the shield itself is likely to affect measured temperatures, and consequently, the accuracy of the measurements (Maclean et al., 2021). The effect is expected to be largest when direct sunlight is at its strongest (during solar noon and summer solstice) and wind speed is low. In the north where the solar angle is relatively low, early summer measurements can be affected by reflected short-wave radiation from the snow-covered surface. To mitigate these potential issues in our temperature data, we defined maximum temperatures (annual and summer) as the 95th percentiles of individual time series. In addition, T2 measurements that represent surface temperatures (Fig. 1c) can be problematic since the proper installation height (+2 cm) is difficult to estimate in the field, particularly in areas with herbaceous vegetation and bryophytes. Therefore, we present the results of T1, T3 and T4 in the main text, and use T2 temperature data only to calculate periods of snow cover (see 2.5.).

2.5. Soil moisture and snow cover

We used monthly soil moisture as a predictor of monthly microclimate temperatures (see 2.7.). Mean monthly soil moisture was calculated from the TMS-4 loggers. The loggers measure soil moisture in the upper 15 cm soil layer and the raw soil moisture count values were transformed to volumetric water content (VWC%) with a calibration function adopted from Wild et al. (2021). Soil moisture measurements were considered only when soil temperature of the same logger was above 1 °C. To impute soil moisture for the missing months (mainly in

winter), we used the value of the last month with sufficient soil moisture data. If this was not possible, we modeled the local soil moisture based on measurements at the focal site of other years (2019–2021) and all data from all other loggers within the study area by fitting a linear mixed effect model, in which we included the month and year as factor predictors and the study site as a random factor. This model was then used for predicting the missing monthly values.

Snow cover duration was also used for predicting monthly microclimate temperatures (see Section 2.7.). It was determined from the surface temperatures (T2) of the TMS-4 loggers by counting the days when the maximum surface temperature stayed below 1°C and the diurnal temperature range was below 10°C calculated with a 10-day moving average. The outcome was visually checked, and the algorithm was considered to detect periods of snow cover well in general. We identified three wetland study sites in the TII study area where the top peat layer stayed so warm under the snow that the automatic snow cover detection failed. For these sites, we identified the snow-covered period visually from the temperature time series. Missing values in snow cover duration were imputed in a similar way to the soil moisture values with the following differences: a generalized linear mixed effect model was used with Poisson distribution and only year was included as a factor predictor. The exact method and code to calculate the snow cover duration are available at the study-area-specific Github repositories (https://github.com/poniitty?tab=repositories).

2.6. Geospatial data

We utilized a multitude of geospatial datasets to derive variables that represent the major environmental drivers hypothesized to affect microclimate temperatures in boreal and tundra biomes. We used airborne light detection and ranging (LiDAR) data, which was provided by the National Land Survey of Finland (https://www.maanmittauslaitos.fi/en/maps-and-spatial-data/expert-users/product-descriptions/laser-scanning-data). The LiDAR data was collected over summers 2016-2019. The point density is ~0.5p/m^2, the standard error of the elevation accuracy is at maximum 15 cm, and the standard error in horizontal accuracy 60 cm. We downloaded a canopy height model produced by the Finnish Forest Center at 1-m spatial resolution (https://www.metsakeskus.fi/fi/avoin-metsa-ja-luontotieto/aineistot-paikkatieto-ohjelmille/paikkatietoaineistot). It is based on the same LiDAR datasets introduced above. We also downloaded and utilized the Finnish national Topographic database which contains e.g., all water bodies, rivers, and wetlands in vector format (https://www.maanmittauslaitos.fi/en/maps-and-spatial-data/expert-users/product-descriptions/topographic-database).

We constructed eight predictors that represent the main aspects of topography, solar radiation, vegetation, and land cover types that are known to affect microclimate temperature (e.g., Ashcroft and Gollan, 2013; Aalto et al., 2017a; Greiser et al., 2018). Topographic predictors, i.e., elevation, potential incoming solar radiation (PISR), and topographic position index (TPI), represent the available energy and cold air pooling capacity. Vegetation effects were represented by canopy cover as high and dense vegetation shades the ground and slows down air movement. Wetland and water body proportions in the surroundings were included to represent their potential buffering effect on temperatures. Additionally, we included the mean soil moisture and snow cover duration calculated from the TMS-4 loggers as predictors.

A Digital Terrain Model (DTM) was produced for each study area based on the LiDAR datasets using the grid_terrain function from the lidR R library (Roussel et al., 2020). The DTM represents elevation at 2-m spatial resolution. These DTMs were then used to calculate potential incoming solar radiation (PISR) for the 15th day of each calendar month using the Potential Incoming Solar Radiation tool in the SAGA-GIS software (version 7.6.2; http://www.saga-gis.org/saga_tool_doc/7.6.2/ta_lighting_2.html). TPI describes the difference in elevation between a focal location and the mean surrounding elevation which we defined with a 100-m radius. TPI was calculated using the Topographic Position Index tool in SAGA-GIS (http://www.saga-gis.org/saga_tool_doc/7.6.2/ta_morphometry_18.html). Canopy cover was calculated from the canopy height model as a proportion of vegetation higher than two meters within a five-meter buffer around the focal location. We extracted still water bodies and wetland land cover polygons from the topographic database (scale 1:10 000), and then calculated the proportion of these land cover types using a 1000 m or 100 m buffer, respectively for each logger location.

2.7. Statistical modeling of monthly microclimate temperatures

We used multivariate statistical modeling to investigate environmental drivers of the monthly microclimate temperatures, as detailed below:

2.7.1. Response variables

We aggregated the quality-checked temperature time series to monthly means (Tavg), maximums (Tmax) and minimums (Tmin). We used the 95th percentile to calculate Tmax, as we expected this to dilute the potential effect of unrealistically high individual measurements caused by the radiation shield. The three measurement heights (i.e., T1, T3, T4), three summary statistics (Tavg, Tmax, Tmin), and 12 months led to a total of 108 response variables.

2.7.2. Predictors

We included the eight predictors (i.e., elevation, PISR, TPI, canopy cover, wetlands, waterbodies, mean soil moisture and snow cover duration) in the models to explain variation in the response variables. However, as the conditions of the seven focus areas contrast greatly, we used a slightly different set of predictors for each area to facilitate model realism. For example, in winter 2019–2020 there was no permanent snow cover in Southern Finland and thus the snow variable was omitted in the model of KAR. Snow cover was also omitted from monthly models for other areas when all study locations were snow free for the whole month. KAR, HYY, and TII show minimal variation in elevation (Table 1). From the initial model results, we noticed that these short elevational gradients resulted in unrealistic model estimates for elevation, and thus, it was omitted from the models for these areas. Furthermore, the proportion of water bodies was not included in VAR, because this focus area has no lakes.

2.7.3. Multivariate modeling

We related the response variables to the predictors by fitting linear models separately for each month and focus area. We considered only linear terms of the eight predictors, because we did not expect strong nonlinear responses, and to avoid the risk of overfitting. After running a full model with all the relevant predictors included, we ran a step function to select the best model based on the AIC value with a both backward and forward mode of stepwise search. As a measure of variable importance, we compared the explanatory power (R^2) of the final model to a model in which the focal predictor was randomly permuted with the vi function from vip R library (Greenwell and Boehmke, 2020). This function also determines the direction of the effect for each predictor based on the sign of the t-statistic, which is analogous to the sign of the slope parameter in regression analysis. If the permuted predictor is important, the R^2 will drop greatly leading to a high importance value. The overall explanatory power of the model is also reflected in the variable importance scores as the drop in R^2 cannot be high if the R^2 is low in the first place. This also gives less weight for poorly performed models when the results are compared or summarized.

3. Results

3.1. Environmental gradients

Our microclimate station network across the seven focus areas covers large environmental gradients (Fig. 2; Table S2) with e.g., elevation ranging from 32 to 934 meters and snow cover duration from 0 to 262 days (KAR to AIL). In most areas, canopy cover ranges from 0 to 100%.

3.2. Spatio-temporal variability in microclimate temperatures

The data demonstrate pronounced spatio-temporal variations in the microclimate temperatures (Figs. 3; S6; Table 2). The intra-annual variation in near-surface (T3) and air temperatures (T4) over all stations was large across the focus areas, for example 64.5°C and 69.3°C in MAL (tundra), and 61.3°C and 54.7°C in HYY (southern-boreal forest), respectively. These microclimate temperature variations often exceeded the variability measured by the adjacent AWS (Table 2). In general, the amplitude of intra-annual soil temperature (T1) variation was ca. 50% of the amplitude of T3 and T4 with the largest variation measured in tundra (ca. 42.1°C; MAL) and the smallest variation in the middle boreal forest (ca. 22.3°C; PIS). Spatial variation in the microclimate temperatures was pronounced both within and among focus areas as well as across seasons (Fig. 4).

The results demonstrate large instantaneous, within-area thermal heterogeneity (Figs. 3; S6; Table 2). For T3, the maximum instantaneous difference across all loggers within each focus area ranged from 17.8 °C (KAR, median=3.3°C) to 32.3°C (MAL, 6.5°C). In the tundra, the largest within-area differences occurred mainly during the snowmelt season (late spring–early summer). In the southern focus areas (HYY and KAR), the magnitude of the thermal heterogeneity in T3 remained fairly constant throughout the year. Thermal heterogeneity in T1 was markedly suppressed during the snow cover period, especially in the northern focus areas (difference ranging from 7.3°C [MAL, median=5.1°C] to 12.4°C [AIL, 6.9°C]). The maximum instantaneous difference in T1 was largest in the tundra (27.1°C [MAL, 5.9°C] and 23.5°C [AIL, 6.7°C]) and smallest in the southern boreal zone (10.1°C in PIS, 2.9°C). Wintertime instantaneous differences in T4 were clearly largest in topographically heterogeneous tundra areas with the difference ranging from 17.5°C (AIL, 3.0°C) to 25.6°C (MAL, 4.2°C; Fig. S6; Table 2). In contrast, during summer, maximum thermal heterogeneity was similar among the tundra and boreal focus areas, but the median heterogeneity was highest in the southernmost focus areas (HYY and KAR).

3.3. Environmental drivers of the temperature variability

The performance of the monthly microclimate models was generally good but varied considerably across seasons and focus areas. The average model fit (R^2) for T1 was 0.44 (minimum R^2 was 0.00 and maximum 0.87), 0.50 (0.00–0.99) for T3, and 0.57 (0.00–0.99) for T4. On average, the Tmax models performed the best (0.53; 0.00–0.99), followed by Tavg (0.51; 0.05–0.96) and Tmin (0.49; 0.00–0.89). More detailed information about the R^2 values is presented in Fig. S7 and Table S3.

Statistical modeling indicated that the drivers of microclimate temperatures vary across months and focus areas (Fig. 5). Overall, canopy

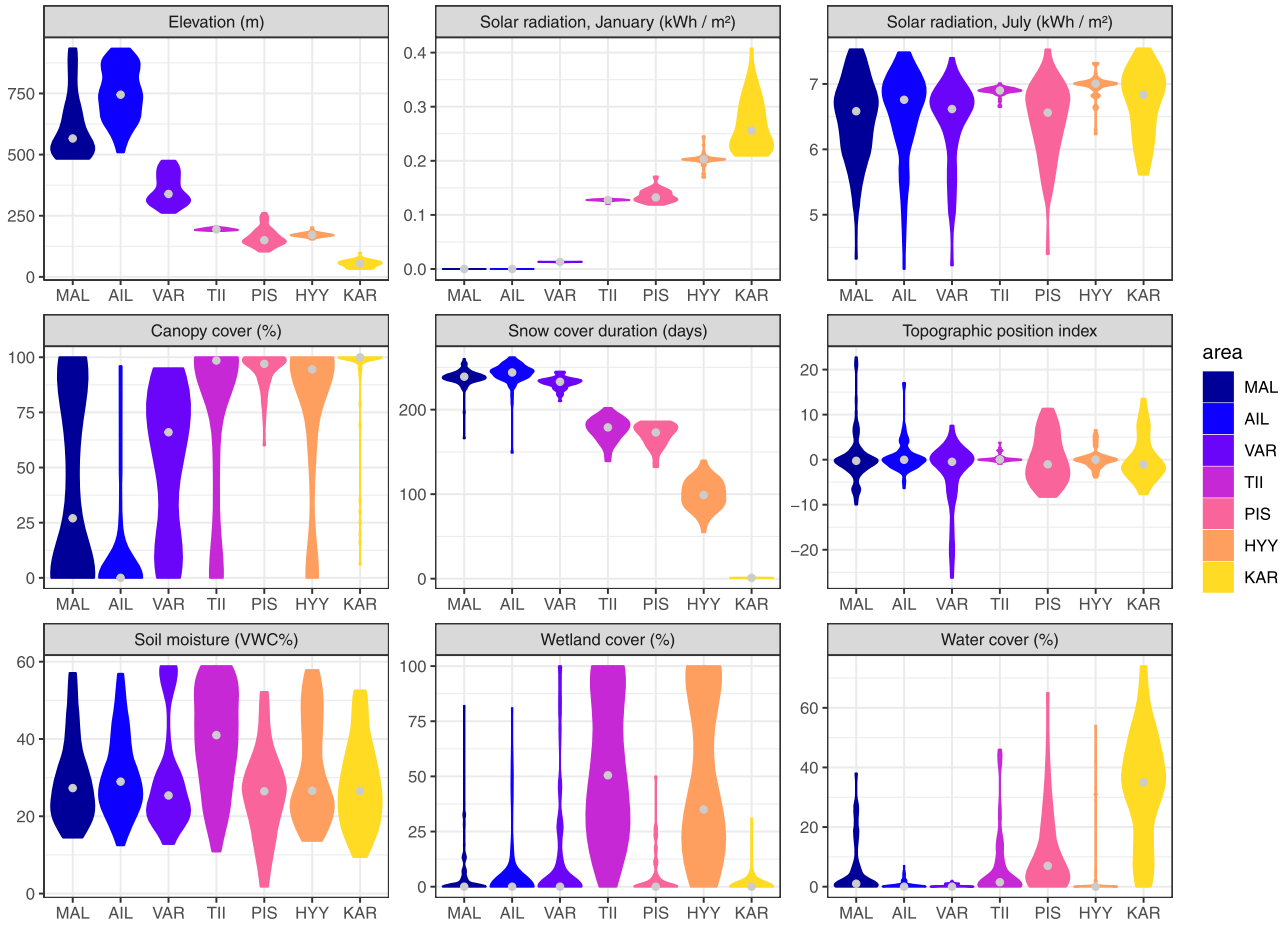

Fig. 2. Environmental gradients covered by the microclimate station network. The figure represents the variability in environmental conditions within the seven focus areas (see Table 1 for the abbreviations). Gray dots depict median values. These environmental variables were used as predictors of the monthly microclimate temperatures.

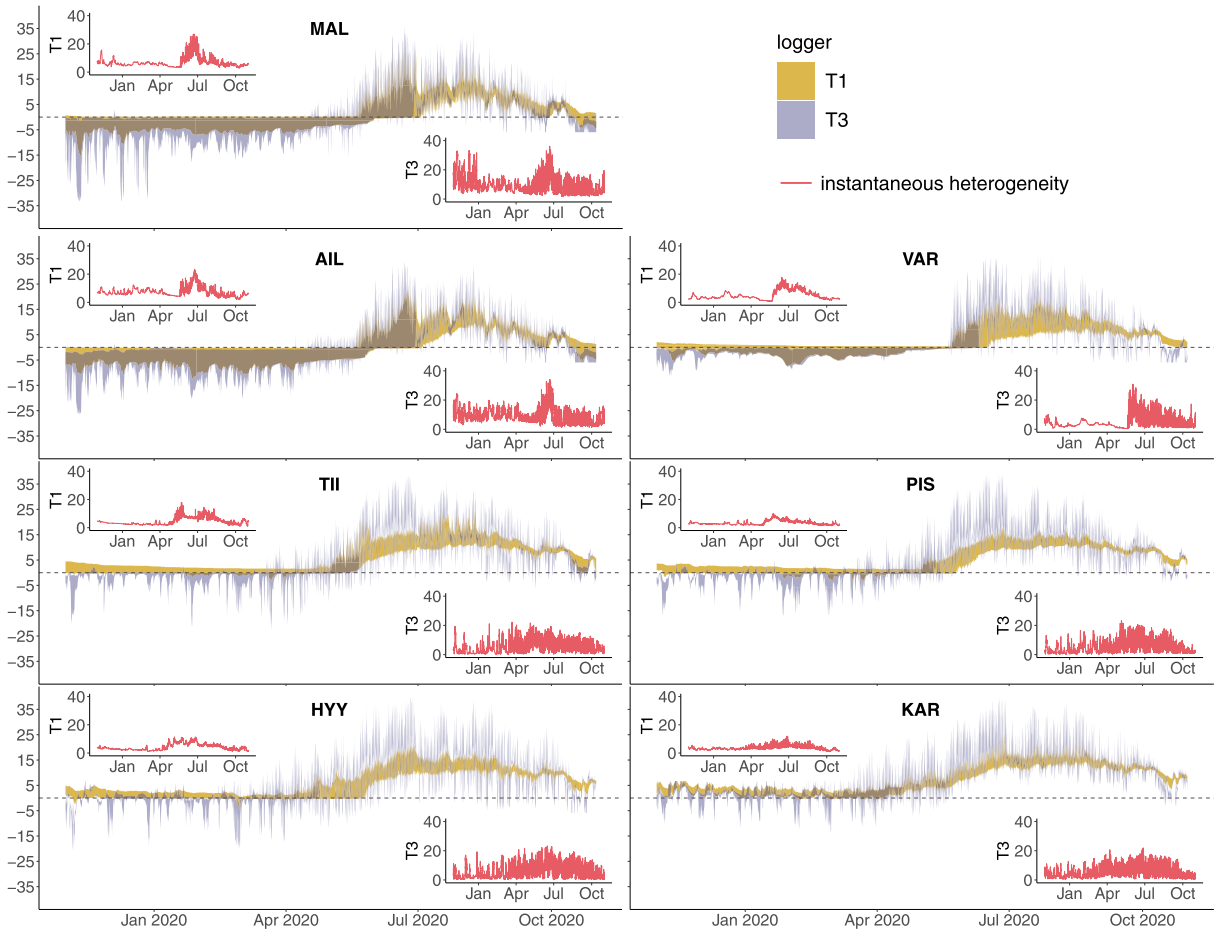

Fig. 3. Spatio-temporal variability of soil and near-surface temperatures in the focus areas. The polygons represent hourly temperature variability over the microclimate stations (number of stations 50–100 per focus area, see Table 1) at two heights, soil temperature (T1) and near-surface temperature (T3), over the study period 2019/11/01–2020/10/31. In the sub-panels, red lines show the maximum instantaneous temperature difference within a given focus area (i.e., thermal heterogeneity, numerical results in Table 2).

Table 2

Intra-annual temperature range of microclimate temperatures and thermal heterogeneity over each focus area. Temperature range over all microclimate stations within a focus area was determined for three measurement heights (T1, T3, and T4 for soil, near-surface, and air temperatures, respectively) and adjacent automated weather stations (AWS). Instantaneous thermal heterogeneity depicts the maximum (median in brackets) within-area temperature difference at a given time.

	Temperature range (°C)				Instantaneous thermal heterogeneity (°C)								
	Intra-annual				Annual			January			July		
Area	*T1*	*T3*	*T4*	*AWS*	*T1*	*T3*	*T4*	*T1*	*T3*	*T4*	*T1*	*T3*	*T4*
MAL	42.1	64.5	69.3	57.2	27.1 (5.9)	32.3 (6.5)	25.6 (4.5)	7.3 (5.1)	17.5 (8.2)	25.6 (4.2)	20.13 (8.3)	16.6 (5.5)	11.0 (3.7)
AIL	35.6	56.9	64.7	57.2	23.5 (6.7)	30.8 (6.4)	21.1 (4.1)	12.4 (6.9)	20.1 (10.0)	17.5 (3.0)	16.4 (9.3)	16.5 (4.0)	12.5 (3.7)
VAR	27.6	49.3	66.0	54.1	17.8 (3.9)	28.2 (2.9)	22.8 (3.2)	8.2 (3.7)	7.7 (2.8)	22.8 (3.4)	14.0 (9.5)	16.3 (4.7)	12.8 (3.5)
TII	29.1	60.8	61.8	53.6	18.0 (3.3)	22.2 (3.3)	16.3 (2.2)	3.8 (2.6)	21.3 (2.6)	9.4 (1.1)	14.2 (8.5)	13.7 (5.1)	10.0 (4.0)
PIS	22.3	54.2	51.1	52.8	10.1 (2.9)	19.0 (3.1)	11.8 (2.2)	4.3 (2.7)	16.7 (2.6)	4.9 (1.5)	6.4 (4.4)	13.2 (4.3)	9.0 (3.5)
HYY	26.1	61.3	54.7	45.4	11.5 (3.3)	20.7 (3.6)	16.7 (2.6)	3.4 (2.3)	12.8 (2.7)	5.6 (1.5)	7.9 (5.6)	15.4 (5.4)	13.1 (4.8)
KAR	28.5	52.1	48.4	37.6	12.0 (3.3)	17.8 (3.3)	12.7 (2.4)	4.2 (3.2)	11.1 (3.6)	5.4 (1.6)	8.2 (4.8)	11.4 (3.7)	10.7 (4.6)

cover was identified as the most important variable in summer (May–August) and elevation in winter and shoulder seasons (September–April). In general, the relative importance of elevation and snow increased by latitude, whereas canopy cover had the largest influence in the southernmost focus areas. As expected, water-related variables were found to be important in study areas with extensive wetlands and lakes.

The direction of the effect of canopy cover on temperatures was dependent on measurement height, response variable, and season (Tables S4–S6). For example, in winter, soil temperatures were consistently higher under closed canopies, whereas in summer the direction was reversed. In turn, T3 and T4 minimum temperatures were higher and maximum temperatures lower under canopies throughout the year, but for average temperatures the sign of the effect varied among seasons. Soil temperatures were consistently warmer under a thick snowpack (indicated by long snow cover duration), but during late spring, the sign of the effect turned opposite when slowly melting snow patches kept soil temperatures colder compared to the rest of the landscape. Snow also had a strong effect on near-surface temperatures by

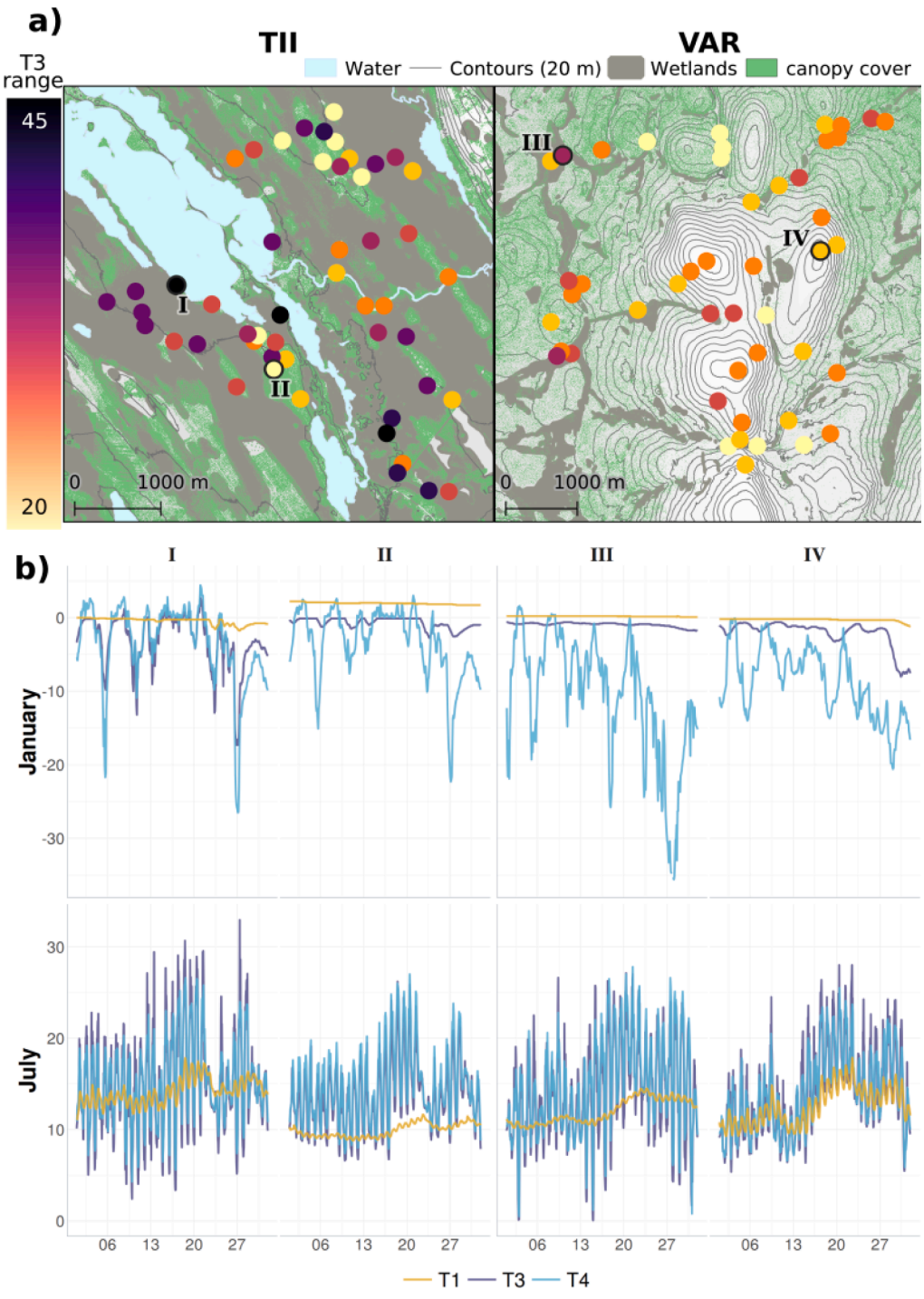

Fig. 4. Microclimate temperature variability over two example focus areas. Panel **a** depicts intra-annual near-surface temperature (T3) variation over the microclimate stations in middle boreal forest (TII) and boreal forest-tundra (VAR). In TII, the intra-annual range in T3 was larger in open measurement sites (nearly 40°C), whereas in forested sites the variation was mostly below 30 °C. In VAR, the largest intra-annual range in T3 was found in open wetland areas (> 40 °C), while areas with least annual variation were located either in forests or in depressions between fells (< 20 °C). Canopy cover represents over 2 m heigh trees. Panel **b** shows January and July temperature time series from example microclimate stations (I–IV in panel **a**). The smallest temperature variations over both focus areas were found in forested sites (II and IV).

increasing Tmin and Tavg and decreasing Tmax. Elevation had, in general, a strong negative effect on temperatures, but especially minimum T4 temperatures showed strong contrasting effects throughout the year.

4. Discussion

4.1. Magnitude of thermal heterogeneity

Our data revealed substantial spatio-temporal variations in microclimate temperatures with distinct landscape and seasonal patterns. Overall, the largest variation in soil and air temperatures was observed in the tundra, where local variability in topography, snow cover, vegetation, and soil moisture create a fine-scale mosaic of thermal conditions (Daly et al., 2010; Scherrer and Körner, 2011; Aalto et al., 2013; Niittynen et al., 2020). This high thermal variability was poorly represented by adjacent AWS that often indicated lower ranges for air temperatures compared to our measurements. Thus, these results provide support for the argument that weather stations insufficiently capture the range of thermal conditions over heterogeneous landscapes, which limits their usability in assessing local climate change impacts (Graae et al., 2012; Lembrechts et al., 2019). We also found that thermal heterogeneity within boreal and tundra landscapes varies markedly at monthly and shorter timescales, with the largest instantaneous differences often

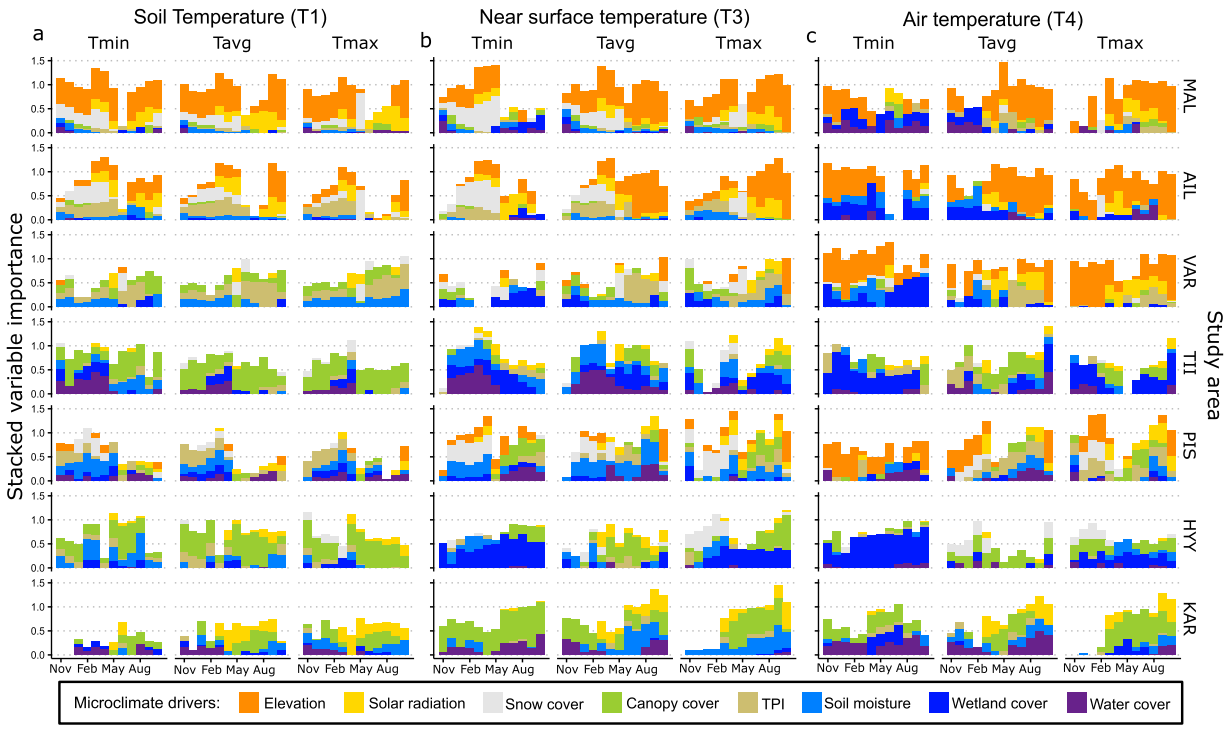

Fig. 5. Relative influence of the environmental drivers explaining monthly microclimate temperature variability. Stacked variable importance scores of the predictors in monthly temperature models per temperature variable (Tmin, Tavg, Tmax) for the three measurement heights (T1, T3, and T4) and for the seven study areas from north (MAL) to south (KAR). Response variables in the models were the monthly minimum (Tmin), average (Tavg) and maximum temperatures (Tmax). Height of the stacked bars also indicate the model fit i.e., a short bar means that the model explained only a little of the temperature variation. TPI = Topographic position index.

exceeding 30°C near the ground (Fig. 3). This heterogeneity was particularly evident in the tundra in early summer during the time of partial snow melt over the landscape. Similar patterns, but in smaller magnitudes, were also detectable in soil temperatures. While the soil temperature heterogeneity during winter was relatively low, the near-surface heterogeneity remained high during winter over most focus areas. This is likely due to fine-scale variation in snow accumulation, which in the studied tundra systems is related to complex topography and in boreal forests to canopy interception (Hedstrom and Pomeroy, 1998; Niittynen et al., 2020). As microclimate is typically not examined over different environments and large extents, these thermal differences have remained undetected (Aalto et al., 2013; Kemppinen et al., 2021). However, our comprehensive study design covering broad geographical and environmental gradients enabled us to quantify the magnitude of thermal heterogeneity and its drivers across distinct ecosystems and landscapes.

4.2. *Drivers of the microclimate temperatures*

Our results show that the main drivers of microclimate temperatures vary over landscapes and seasons. For example, in the northernmost focus areas in the oroarctic tundra, the elevational gradient clearly has the largest influence, especially on the above-surface temperatures via the atmospheric lapse rate. Also, the role of local topography is particularly evident in the tundra, where it drives microclimate temperature variability by controlling surface net radiation and cold-air pooling (e.g., Daly et al., 2010; Dobrowski, 2011). In addition, local topography controls spatial snow patterns and soil moisture, which are among the key factors creating thermal heterogeneity close to the soil surface and controlling many ecosystem processes (Aalto et al., 2013; le Roux et al., 2013; Niittynen et al., 2020). In our study design, local elevational differences diminish towards the southernmost focus areas, and consequently, the relative importance of other microclimate drivers increases. For example, our data reveal that canopies, water bodies, and wetlands can create larger maximum and average thermal heterogeneity in air temperatures in forests than observed in the tundra. Forest canopy is especially important in the southernmost focus areas where dense canopies decrease the maximum, but increase the minimum temperatures, which leads to buffered thermal conditions compared to open areas. Importantly, our analyses show how the role of microclimatic drivers is dependent on their landscape structuring and amount of variability. For example, this suggest that in other tundra regions with less topographical heterogeneity compared to our focus areas other factors such as vegetation or water bodies are likely to be more important drivers of microclimate temperature than e.g., elevation and local topographical gradients.

Our data show that drivers of temperature variability are also dependent on the height from the surface (De Frenne et al., 2021; Maclean and Klinges, 2021). This is demonstrated by the effect of canopy cover – a dense canopy buffers air and near-surface temperature variation whereas soil temperatures follow a distinct seasonal cycle where minimum, maximum, and mean temperatures are all consistently lower in forests in summer but higher in winter compared to open areas (in agreement with De Frenne et al., 2019). In our data, soil temperatures were decoupled from elevational gradients, and, on average, elevation had the greatest importance for air temperatures. This is especially evident in the tundra, where temperatures at 150 cm are less affected by heterogeneous surface conditions and are more dependent on meso- and macro-scale topographical gradients (Aalto et al., 2017a; Maclean et al., 2019). During the study period, temperature inversions in the lower atmosphere were so prevalent in our northernmost focus areas that even the monthly mean air temperatures positively correlated with elevation during some winter months. This is not evident in the near-surface temperatures recorded under snow. In general, soil temperatures had similar driver contributions in minimum, maximum and mean temperatures. Whereas, for near-surface and air temperatures,

minimum and maximum temperatures often had contrasting variable importances and effects. This is probably because soil temperatures are less affected by short-term variability in weather and radiation conditions, and thus, minimums and maximums are more closely coupled in soil temperatures than in air (Ashcroft and Gollan, 2013). These height-dependent patterns that we found highlight the importance of considering vertical temperature gradients when analyzing microclimatic heterogeneity in space and time.

4.3. Methodological uncertainties

Statistical modeling of microclimates can be challenging, as the same variables and model parameters proposed for one location and time may not be applicable for other areas and seasons. Temperature variation follows physical principles but the commonly used geospatial predictors are usually proxies for the underlying mechanisms (e.g., topographic position, proximity to water bodies and wetlands). The quality and representativeness of such predictors is crucial when interpreting the modeling results. Here, we aimed to evaluate the area-specific strength of the statistical links between the predictors and the microclimate temperatures rather than to produce accurate spatially explicit predictions. Most of the statistical relationships were logical except for few individual results. For example, the models suggested that increasing wetland cover decreased the minimum and increased the maximum air temperatures in our data throughout the year, while in theory, a large water body should have the opposite effect, especially during the snow and ice-free season. However, in our data the wetland cover was negatively correlated with canopy cover in many of the focus areas (the smallest Spearman correlation coefficient was -0.71), which may confound the found effects. Furthermore, wetlands are typically located in topographic depressions, and thus, wetlands may be better proxies for cold air pooling potential than a topographic position index (TPI). Mechanistic microclimate models are increasingly developed and can solve some of these problems, but they are similarly dependent on the input data quality and can also be computationally demanding when applied over large extents at high spatial resolution (Maclean et al., 2019). More research is needed to improve the quality of the geospatial data fed into statistical and mechanistic microclimate models.

Measuring microclimate temperatures is prone to errors as the processes creating measurement errors are the same as those responsible for creating the thermal variation (e.g., incoming solar radiation, air mixing; Maclean et al., 2021). This is of particular concern for temperature measurements conducted above the ground surface and if the sensors are exposed to sunlight. Consequently, the sensors themselves can heat up, and the temperature recordings of ambient conditions can be substantially overestimated. Radiation shielding around the sensors is commonly used to mitigate the issue, but the choice of shielding (e.g., material, structure) is not trivial (Maclean et al., 2021). In future studies, these measurement errors could be accounted for by, for instance, quantifying the possible errors across seasons (e.g., snow covered and bare ground), landscapes (contrasting expositions), and weather conditions. Solving such practical methodological challenges is especially timely as new microclimate networks are emerging (e.g., Greiser et al., 2018; Lembrechts et al., 2020) to facilitate more accurate predictions of future microclimates and associated ecosystem impacts.

4.4. Future microclimate temperatures and ecosystem implications

Since the preindustrial time, the macroclimate has warmed 2.3°C over the study domain with pronounced observed and predicted changes in thermal seasons, precipitation, and snow cover (Mikkonen et al., 2015; Bintanja and Andry, 2017; Ruosteenoja et al., 2016, 2019; Luomaranta et al., 2019). However, microclimates may not directly follow changes in macroclimate due to the differing dynamics of the environmental drivers and how they are structured over landscapes (e.g., Maclean et al., 2016; Aalto et al., 2018; De Frenne et al., 2019). For example, elevation gradients and local topography as static drivers will create thermal heterogeneity also in the future (Daly et al., 2010; Dobrowski, 2011). In turn, climate warming has already delayed lake freeze-up and advanced ice break-up (Newton and Mullan, 2021), which can affect microclimates of adjacent areas due to prolonged ice-free periods that sustain the energy exchange between lake and atmosphere (Brown and Duguay, 2010). Changes in wetlands' water balance (due to drainage and restoration) influence their thermal properties, energy fluxes, and biogeophysical feedbacks that can lead to altered local temperature variability (Menberu et al., 2016; Laine et al., 2019; Fernández-Pascual and Correia-Álvarez, 2021; Słowińska et al., 2022).

In the tundra, changes in snow cover and properties control temporal dynamics and magnitude of landscape level thermal heterogeneity, especially close to the soil surface (Aalto et al., 2018; Niittynen et al., 2020). Shortening of the snow season could translate into earlier peaks in landscape thermal heterogeneity and a general shift towards more thermally homogeneous tundra landscapes. Changes in snow cover could also lead to alterations in e.g., permafrost conditions by enabling deeper seasonal thaw (Stieglitz et al., 2003). In addition, the expansion of shrub vegetation to tundra as a response to climate warming have been widely observed (e.g., Sturm et al., 2001; Tape et al., 2006). These changes in vegetation communities and their structure may have significant effects on tundra microclimates via e.g., trapping snow, incepting radiation, and altering biophysical feedbacks (Myers-Smith et al., 2011; Mekonnen et al., 2021). In both biomes, abiotic and biotic disturbances, such as windstorms, wildland fires, and pest outbreaks, can lead to changes in local temperatures due to their effect on e.g., vegetation structuring that in turn controls many of the microclimatic processes (Venäläinen et al., 2020; De Frenne et al., 2021).

Microclimates and their changes have implications for the ecology and functioning of boreal and tundra environments due to the inherent linkages to the organisms' performance and ecosystem processes (Maclean et al., 2016; Körner and Hiltbrunner, 2018; Bentz et al. 2019; Zellweger et al., 2020; Seibold et at., 2021). However, mostly due to a lack of observation data such links have been anticipated rather than directly detected (De Frenne and Verheyen, 2016). It is only with contemporary developments in data loggers and remote sensing (e.g., light detection-and-ranging, LiDAR) that extensive mapping of canopy structures and microclimates has become a reality (Lenoir et al., 2017; Zellweger et al., 2019; Leipe and Carey, 2021). Using microclimate data will allow more organism-centered approaches to determine species range boundaries and related climate change dynamics (Potter et al., 2013; Bentz et al., 2019). For example, microclimate could be incorporated into investigations of the temperature-driven leading and trailing edges, where species' responses may be susceptible to the availability of suitable microclimate and associated microrefugia (Hylander et al., 2015; Keppel et al., 2015). Moreover, a landscape with various microclimates is also likely to transition slower to an alternate state, whereas a landscape with homogeneous microclimate may transition due to minor temperature shifts in the macroclimate (Randin et al., 2009; Lenoir et al., 2013; Aalto et al., 2018). Therefore, thermally heterogeneous landscapes could be more resilient against climate changes and short-term climate extremes (e.g., drought), and recover faster and/or persist better in response to perturbations than their low resilience counterparts (Kühsel and Blüthgen, 2015). With further expansions, our comprehensive study setting could also provide possibilities to analyze, model, and compare the effects of microclimate on ecosystem functioning of pristine and managed boreal forests. This is relevant, since different forest types and management practices can produce substantial near-ground microclimate variation (De Frenne and Verheyen, 2016; Greiser et al., 2018).

5. Conclusions

We showed remarkable multi-level microclimate temperature variability over boreal forest and tundra biomes based on the data from

hundreds of microclimate stations. The data revealed high instantaneous thermal heterogeneity over the landscapes, with the largest differences found in the tundra during wintertime and in southern boreal forest during summer. Our results suggested that microclimate temperature variability in southern boreal forests is mostly driven by canopy cover and proximity of water covers. In the tundra, the microclimatic temperature variability is most strongly linked to the elevation gradient, variations in topographic solar radiation and snow cover. Here we have also showed that the relative importance and effects of microclimate drivers and landscape thermal heterogeneity vary seasonally. This calls for careful investigation of the temporal aspects in future microclimate studies. As microclimate temperatures are the most proximally related to organisms' performance and various ecosystem functions, our new comprehensive data will be highly relevant in various ecosystem applications aiming to understand and project the biome-wide responses to contemporary climate change.

Data availability

The raw microclimate data and code to preprocess these data are available in the study-area-specific Github repositories (https://github.com/poniitty?tab=repositories). The preprocessed data and code used in this study are available in a Github repository (https://github.com/poniitty/Boreal-Tundra_Microclimates) and a static version of this repository will be deposited and openly published in Zenodo upon acceptance for publishing.

Declaration of Competing Interest

The authors declare no conflict of interests.

Acknowledgements

JA and HG acknowledges Academy of Finland Flagship funding (Grant No. 337552), and JA and VT acknowledge the funding by the Faculty of Science, University of Helsinki (project MICROCLIM, grant no. 7510145). JK was funded by the Arctic Interactions at the University of Oulu and Academy of Finland (Grant No. 318930, Profi 4). TR was funded by the Doctoral programme in Geosciences at the University of Helsinki. PN was funded by the Nessling Foundation and the Kone foundation. We want to thank all field work assistants and the staff of Värriö, Hyytiälä and Kilpisjärvi research stations. We acknowledge funding from Nordenskiöld samfundet, Tiina and Antti Herlin foundation, Oskar Öflunds stiftelse, and Maa- ja vesitekniikan tuki ry.

Supplementary materials

Supplementary material associated with this article can be found, in the online version, at doi:10.1016/j.agrformet.2022.109037.

References

Aalto, J., le Roux, P.C., Luoto, M., 2013. Vegetation mediates soil temperature and moisture in arctic-alpine environments. Arctic Antarctic Alpine Res. 45 (4), 429–439. https://doi.org/10.1657/1938-4246-45.4.429.

Aalto, J., Riihimäki, H., Meineri, E., Hylander, K., Luoto, M., 2017a. Revealing topoclimatic heterogeneity using meteorological station data. Int. J. Climatol. 37 (S1), 544–556. https://doi.org/10.1002/joc.5020.

Aalto, J., Harrison, S., Luoto, M., 2017b. Statistical modelling predicts almost complete loss of major periglacial processes in Northern Europe by 2100. Nat. Commun. 8 (1), 515. https://doi.org/10.1038/s41467-017-00669-3.

Aalto, J., Scherrer, D., Lenoir, J., Guisan, A., Luoto, M., 2018. Biogeophysical controls on soil-atmosphere thermal differences: Implications on warming Arctic ecosystems. Environ. Res. Lett. 13 (7), 074003 https://doi.org/10.1088/1748-9326/aac83e.

Ashcroft, M.B., Gollan, J.R., 2013. Moisture, thermal inertia, and the spatial distributions of near-surface soil and air temperatures: Understanding factors that promote microrefugia. Agric. For. Meteorol. 176, 77–89. https://doi.org/10.1016/j.agrformet.2013.03.008.

Barry, R., Blanken, P., 2016. Microclimate and Local Climate. Cambridge University Press, Cambridge.

Bedia, J., Herrera, S., Gutiérrez, J.M., 2013. Dangers of using global bioclimatic datasets for ecological niche modeling. Limitations for future climate projections. Global Planet. Change 107, 1–12. https://doi.org/10.1016/j.gloplacha.2013.04.005.

Bentz, B.J., Jönsson, A.M., Schroeder, M., Weed, A., Wilcke, R.A.I., Larsson, K., 2019. *Ips typographus* and *Dendroctonus ponderosae* models project thermal suitability for intra- and inter-continental establishment in a changing climate. Front. For. Glob. Change 2 (1). https://doi.org/10.3389/ffgc.2019.00001.

Bintanja, R., Andry, O., 2017. Towards a rain-dominated arctic. Nat. Clim. Change 7 (4), 263–267. https://doi.org/10.1038/nclimate3240.

Brown, L.C., Duguay, C.R., 2010. The response and role of ice cover in lake-climate interactions. Prog. Phys. Geogr. 34 (5), 671–704. https://doi.org/10.1177/0309133310375653.

Daly, C., Conklin, D.R., Unsworth, M.H., 2010. Local atmospheric decoupling in complex topography alters climate change impacts. Int. J. Climatol. 30 (12), 1857–1864. https://doi.org/10.1002/joc.2007.

De Frenne, P., Verheyen, K., 2016. Weather stations lack forest data. Science 351 (6270), 234. https://doi.org/10.1126/science.351.6270.234-a. -234.

De Frenne, P., Zellweger, F., Rodríguez-Sánchez, F., Scheffers, B.R., Hylander, K., Luoto, M., Vellend, M., Verheyen, K., Lenoir, J., 2019. Global buffering of temperatures under forest canopies. Nat. Ecol. Evol. 3 (5), 744–749. https://doi.org/10.1038/s41559-019-0842-1.

De Frenne, P., Lenoir, J., Luoto, M., Scheffers, B.R., Zellweger, F., Aalto, J., Ashcroft, M. B., Christiansen, D.M., Decocq, G., Pauw, K.D., Govaert, S., Greiser, C., Gril, E., Hampe, A., Jucker, T., Klinges, D.H., Koelemeijer, I.A., Lembrechts, J.J., Marrec, R., Hylander, K., 2021. Forest microclimates and climate change: importance, drivers and future research agenda. Glob. Change Biol. 27 (11), 2279–2297. https://doi.org/10.1111/gcb.15569.

Dobrowski, S.Z., 2011. A climatic basis for microrefugia: The influence of terrain on climate. Glob. Change Biol. 17 (2), 1022–1035. https://doi.org/10.1111/j.1365-2486.2010.02263.x.

Du, E., Terrer, C., Pellegrini, A.F., Ahlström, A., van Lissa, C.J., Zhao, X., Xia, N., Wu, X., Jackson, R.B., 2020. Global patterns of terrestrial nitrogen and phosphorus limitation. Nat. Geosci. 13, 221–226. https://doi.org/10.1038/s41561-019-0530-4.

Fernández-Pascual, E., Correia-Álvarez, E., 2021. Mire microclimate: groundwater buffers temperature in waterlogged versus dry soils. Int. J. Climatol. 41 (S1), E2949–E2958. https://doi.org/10.1002/joc.6893.

Fick, S.E., Hijmans, R.J., 2017. WorldClim 2: new 1km spatial resolution climate surfaces for global land areas. Int. J. Climatol. 37 (12), 4302–4315. https://doi.org/10.1002/joc.5086.

Flato, G.M., 2011. Earth system models: an overview. Wiley Interdiscip. Rev. Clim. Change 2 (6), 783–800. https://doi.org/10.1002/wcc.148.

Gardner, A.S., Maclean, I.M.D., Gaston, K.J., 2019. Climatic predictors of species distributions neglect biophysiologically meaningful variables. Divers. Distrib. 25 (8), 1318–1333. https://doi.org/10.1111/ddi.12939.

Graae, B.J., De Frenne, P., Kolb, A., Brunet, J., Chabrerie, O., Verheyen, K., Pepin, N., Heinken, T., Zobel, M., Shevtsova, A., 2012. On the use of weather data in ecological studies along altitudinal and latitudinal gradients. Oikos 121 (1), 3–19. https://doi.org/10.1111/j.1600-0706.2011.19694.x.

Greenwell, B.M., Boehmke, B.C., 2020. Variable importance plots – an introduction to the vip package. R J. 12 (1), 343–366. https://doi.org/10.32614/RJ-2020-013.

Greiser, C., Meineri, E., Luoto, M., Ehrlén, J., & Hylander, K. (2018). Monthly microclimate models in a managed boreal forest landscape. Agric. For. Meteorol., 250, 147–158. 10.1016/j.agrformet.2017.12.252.

Grundstein, A., Todhunter, P., Mote, T., 2005. Snowpack control over the thermal offset of air and soil temperatures in eastern North Dakota. Geophys. Res. Lett. 32 (8) https://doi.org/10.1029/2005GL022532.

Haesen, S., Lembrechts, J.J., De Frenne, P., Lenoir, J., Aalto, J., Ashcroft, M.B., Kopecký, M., Luoto, M., Maclean, I.M.D., Nijs, I., Niittynen, P., van den Hoogen, J., Arriga, N., Brůna, J., Buchmann, N., Čiliak, M., Collalti, A., De Lombaerde, E., Descombes, P., Van Meerbeek, K., 2021. ForestTemp – sub-canopy microclimate temperatures of European forests. Glob. Change Biol. 27 (23), 6307–6319. https://doi.org/10.1111/gcb.15892.

Hattab, T. & Lenoir, J. (2017). iSDM: invasive species distribution modelling. R package version 1.0. https://CRAN.R-project.org/package=iSDM.

Hedstrom, N.R., Pomeroy, J.W., 1998. Measurements and modelling of snow interception in the boreal forest. Hydrol. Proc. 12 (10-11), 1611–1625. https://doi.org/10.1002/(SICI)1099-1085(199808/09)12:10/11≦1611::AID-HYP684≧3.0.CO;2-4.

Hylander, K., Ehrlén, J., Luoto, M., Meineri, E., 2015. Microrefugia: not for everyone. Ambio 44 (1), 60–68. https://doi.org/10.1007/s13280-014-0599-3.

Jokinen, P., Pirinen, P., Kaukoranta, J.P., Kangas, A., Alenius, P., Eriksson, P., Johansson, M., Wilkman, S., 2021. Tilastoja Suomen ilmastosta ja merestä 1991–2020. Ilmatieteen Laitos Finn. Meteorol. Inst. Rap. 2021, 8.

Karger, D.N., Conrad, O., Böhner, J., Kawohl, T., Kreft, H., Soria-Auza, R.W., Zimmermann, N.E., Linder, P., Kessler, M., 2017. Climatologies at high resolution for the Earth land surface areas. Sci. Data 4 (1), 1–12. https://doi.org/10.1038/sdata.2017.122.

Kemppinen, J., Niittynen, P., Virkkala, A.-M., Happonen, K., Riihimäki, H., Aalto, J., Luoto, M., 2021. Dwarf shrubs impact tundra soils: drier, colder, and less organic carbon. Ecosystems 24 (6), 1378–1392. https://doi.org/10.1007/s10021-020-00589-2.

Keppel, G., Mokany, K., Wardell-Johnson, G.W., Phillips, B.L., Welbergen, J.A., Reside, A.E., 2015. The capacity of refugia for conservation planning under climate change. Front. Ecol. Environ. 13 (2), 106–112. https://doi.org/10.1890/140055.

Körner, C., Hiltbrunner, E., 2018. The 90 ways to describe plant temperature. Perspect. Plant Ecol. Evolut. Syst. 30, 16–21. https://doi.org/10.1016/j.ppees.2017.04.004.

Kühsel, S., Blüthgen, N., 2015. High diversity stabilizes the thermal resilience of pollinator communities in intensively managed grasslands. Nat. Commun. 6 (1), 1–10. https://doi.org/10.1038/ncomms8989.

Laine, A.M., Mehtätalo, L., Tolvanen, A., Frolking, S., Tuittila, E.S., 2019. Impacts of drainage, restoration and warming on boreal wetland greenhouse gas fluxes. Sci. Total Environ. 647, 169–181. https://doi.org/10.1016/j.scitotenv.2018.07.390.

Leipe, S.C., Carey, S.K., 2021. Rapid shrub expansion in a subarctic mountain basin revealed by repeat airborne LiDAR. Environ. Res. Commun. 3 (7), 071001 https://doi.org/10.1088/2515-7620/ac0e0c.

Lembrechts, J.J., Lenoir, J., Roth, N., Hattab, T., Milbau, A., Haider, S., Pellissier, L., Pauchard, A., Ratier Backes, A., Dimarco, R.D., Nuñez, M.A., Aalto, J., Nijs, I., 2019. Comparing temperature data sources for use in species distribution models: From in-situ logging to remote sensing. Glob. Ecol. Biogeogr. 28 (11), 1578–1596. https://doi.org/10.1111/geb.12974.

Lembrechts, J.J., Aalto, J., Ashcroft, M.B., De Frenne, P., Kopecký, M., Lenoir, J., Luoto, M., Maclean, I.M.D., Roupsard, O., Fuentes-Lillo, E., García, R.A., Pellissier, L., Pitteloud, C., Alatalo, J.M., Smith, S.W., Björk, R.G., Muffler, L., Ratier Backes, A., Cesarz, S., Nijs, I., 2020. SoilTemp: A global database of near-surface temperature. Glob. Change Biol. 26 (11), 6616–6629. https://doi.org/10.1111/gcb.15123.

Lenoir, J., Graae, B.J., Aarrestad, P.A., Alsos, I.G., Armbruster, W.S., Austrheim, G., Bergendorff, C., Birks, H.J.B., Bråthen, K.A., Brunet, J., Bruun, H.H., Dahlberg, C.J., Decocq, G., Diekmann, M., Dynesius, M., Ejrnaes, R., Grytnes, J.A., Hylander, K., Klanderud, K., Svenning, J.C., 2013. Local temperatures inferred from plant communities suggest strong spatial buffering of climate warming across Northern Europe. Glob. Change Biol. 19 (5), 1470–1481. https://doi.org/10.1111/gcb.12129.

Lenoir, J., Hattab, T., Pierre, G., 2017. Climatic microrefugia under anthropogenic climate change: Implications for species redistribution. Ecography 40 (2), 253–266. https://doi.org/10.1111/ecog.02788.

Luomaranta, A., Aalto, J., Jylhä, K., 2019. Snow cover trends in Finland over 1961–2014 based on gridded snow depth observations. Int. J. Climatol. 39 (7), 3147–3159. https://doi.org/10.1002/joc.6007.

Maclean, I.M.D., Suggitt, A.J., Wilson, R.J., Duffy, J.P., Bennie, J.J., 2016. Fine-scale climate change: modelling spatial variation in biologically meaningful rates of warming. Glob. Change Biol. 23 (1), 256–268. https://doi.org/10.1111/gcb.13343.

Maclean, I.M.D., Mosedale, J.R., Bennie, J.J., 2019. Microclima: An R package for modelling meso- and microclimate. Methods Ecol. Evol. 10, 280–290. https://doi.org/10.1111/2041-210X.13093.

Maclean, I.M.D., Duffy, J.P., Haesen, S., Govaert, S., De Frenne, P., Vanneste, T., Lenoir, J., Lembrechts, J.J., Rhodes, M.W., Van Meerbeek, K., 2021. On the measurement of microclimate. Methods Ecol. Evol. 12 (8), 1397–1410. https://doi.org/10.1111/2041-210X.13627.

Maclean, I.M.D., Klinges, D.H., 2021. Microclimc: a mechanistic model of above, below and within-canopy microclimate. Ecol. Modell. 451, 109567 https://doi.org/10.1016/j.ecolmodel.2021.109567.

McGuire, A.D., Anderson, L.G., Christensen, T.R., Dallimore, S., Guo, L., Hayes, D.J., Heimann, M., Lorenson, T.D., Macdonald, R.W., Roulet, N., 2009. Sensitivity of the carbon cycle in the Arctic to climate change. Ecol. Monogr. 79 (4), 523–555. https://doi.org/10.1890/08-2025.1.

Mekonnen, Z.A., Riley, W.J., Berner, L.T., Bouskill, N.J., Torn, M.S., Iwahana, G., Breen, A.L., Myers-Smith, I.H., Criado, M.G., Liu, Y., Euskirchen, E.S., Goetz, S.J., Mack, M.C., Grant, R.F., 2021. Arctic tundra shrubification: A review of mechanisms and impacts on ecosystem carbon balance. Environ. Res. Lett. 16 (5), 053001 https://doi.org/10.1088/1748-9326/abf28b.

Menberu, M.W., Tahvanainen, T., Marttila, H., Irannezhad, M., Ronkanen, A.-K., Penttinen, J., Kløve, B., 2016. Water-table-dependent hydrological changes following peatland forestry drainage and restoration: analysis of restoration success. Water Resour. Res. 52 (5), 3742–3760. https://doi.org/10.1002/2015WR018578.

Mikkonen, S., Laine, M., Mäkelä, H.M., Gregow, H., Tuomenvirta, H., Lahtinen, M., Laaksonen, A., 2015. Trends in the average temperature in Finland, 1847–2013. Stoch. Environ. Res. Risk Assess. 29 (6), 1521–1529. https://doi.org/10.1007/s00477-014-0992-2.

Newton, A.M.W., Mullan, D.J., 2021. Climate change and Northern Hemisphere lake and river ice phenology from 1931–2005. Cryosphere 15 (5), 2211–2234. https://doi.org/10.5194/tc-15-2211-2021.

Niittynen, P., Heikkinen, R.K., Aalto, J., Guisan, A., Kemppinen, J., Luoto, M., 2020. Fine-scale tundra vegetation patterns are strongly related to winter thermal conditions. Nat. Clim. Change 10 (12), 1143–1148. https://doi.org/10.1038/s41558-020-00916-4.

Pepin, N.C., Schaefer, M.K., Riddy, L.D., 2009. Quantification of the cold-air pool in Kevo Valley, Finnish Lapland. Weather 64 (3), 60–67. https://doi.org/10.1002/wea.260.

Post, E., Forchhammer, M.C., Bret-Harte, M.S., Callaghan, T.V., Christensen, T.R., Elberling, B., Fox, A.D., Gilg, O., Hik, D.S., Høye, T.T., Ims, R.A., Jeppesen, E., Klein, D.R., Madsen, J., McGuire, A.D., Rysgaard, S., Schindler, D.E., Stirling, I., Tamstorf, M.P., Aastrup, P., 2009. Ecological dynamics across the Arctic associated with recent climate change. Science 325, 1355–1358. https://doi.org/10.1126/science.1173113.

Potter, K.A., Woods, H.A., Pincebourde, S., 2013. Microclimatic challenges in global change biology. Glob. Change Biol. 19 (10), 2932–2939. https://doi.org/10.1111/gcb.12257.

Randin, C.F., Engler, R., Normand, S., Zappa, M., Zimmermann, N.E., Pearman, P.B., Vittoz, P., Thuiller, W., Guisan, A., 2009. Climate change and plant distribution: local models predict high-elevation persistence. Glob. Change Biol. 15 (6), 1557–1569. https://doi.org/10.1111/j.1365-2486.2008.01766.x.

Roussel, J.-R., Auty, D., Coops, N.C., Tompalski, P., Goodbody, T.R.H., Meador, A.S., Bourdon, J.F., de Boissieu, F., Achim, A., 2020. lidR: An R package for analysis of Airborne Laser Scanning (ALS) data. Remote Sens. Environ. 251, 112061 https://doi.org/10.1016/j.rse.2020.112061.

Ruosteenoja, K., Jylhä, K., Kämäräinen, M., 2016. Climate projections for Finland under the RCP forcing scenarios. Geophysica 51 (1), 17–50.

Ruosteenoja, K., Markkanen, T., Räisänen, J., 2019. Thermal seasons in northern Europe in projected future climate. Int. J. Climatol. 40 (10), 4444–4462. https://doi.org/10.1002/joc.6466.

le Roux, P.C., Aalto, J., Luoto, M., 2013. Soil moisture's underestimated role in climate change impact modelling in low-energy systems. Glob. Change Biol. 19 (10), 2965–2975. https://doi.org/10.1111/gcb.12286.

Scherrer, D., Koerner, C., 2011. Topographically controlled thermal-habitat differentiation buffers alpine plant diversity against climate warming. J. Biogeogr. 38 (2), 406–416. https://doi.org/10.1111/j.1365-2699.2010.02407.x.

Seibold, S., Rammer, W., Hothorn, T., Seidl, R., Ulyshen, M.D., Lorz, J., Cadotte, M.W., Lindenmayer, D.B., Adhikari, Y.P., Aragón, R., Bae, S., Baldrian, P., Barimani Varandi, H., Barlow, J., Bässler, C., Beauchêne, J., Berenguer, E., Bergamin, R.S., Birkemoe, T., Müller, J., 2021. The contribution of insects to global forest deadwood decomposition. Nature 597 (7874), 77–81. https://doi.org/10.1038/s41586-021-03740-8.

Słowińska, S., Słowiński, M., Marcisz, K., Lamentowicz, M., 2022. Long-term microclimate study of a peatland in Central Europe to understand microrefugia. Int. J. Biometeorol. https://doi.org/10.1007/s00484-022-02240-2.

Soudzilovskaia, N.A., van der Heijden, M.G., Cornelissen, J.H., Makarov, M.I., Onipchenko, V.G., Maslov, M.N., Akhmetzhanova, A.A., van Bodegom, P.M., 2015. Quantitative assessment of the differential impacts of arbuscular and ectomycorrhiza on soil carbon cycling. New Phytol. 208 (1), 280–293. https://doi.org/10.1111/nph.13447.

Suggitt, A.J., Gillingham, P.K., Hill, J.K., Huntley, B., Kunin, W.E., Roy, D.B., Thomas, C. D., 2011. Habitat microclimates drive fine-scale variation in extreme temperatures. Oikos 120 (1), 1–8. https://doi.org/10.1111/j.1600-0706.2010.18270.x.

Stieglitz, M., Déry, S.J., Romanovsky, V.E., Osterkamp, T.E., 2003. The role of snow cover in the warming of arctic permafrost. Geophys. Res. Lett. 30 (13) https://doi.org/10.1029/2003GL017337.

Sturm, M., Racine, C., Tape, K., 2001. Increasing shrub abundance in the Arctic. Nature 411, 546–547. https://doi.org/10.1038/35079180.

Tape, K., Sturm, M., Racine, C., 2006. The evidence for shrub expansion in Northern Alaska and the Pan-Arctic. Glob. Change Biol. 12 (4), 686–702. https://doi.org/10.1111/j.1365-2486.2006.01128.x.

Tikkanen, M., 2005. Climate. In: Seppälä, M. (Ed.), The physical geography of Fennoscandia. Oxford University Press, Oxford.

Venäläinen, A., Lehtonen, I., Laapas, M., Ruosteenoja, K., Tikkanen, O.P., Viiri, H., Ikonen, V.P., Peltola, H., 2020. Climate change induces multiple risks to boreal forests and forestry in Finland: a literature review. Glob. Change Biol. 26 (8), 4178–4196. https://doi.org/10.1111/gcb.15183.

Virkkala, A.-M., Aalto, J., Rogers, B.M., Tagesson, T., Treat, C.C., Natali, S.M., Watts, J. D., Potter, S., Lehtonen, A., Mauritz, M., Schuur, E.A.G., Kochendorfer, J., Zona, D., Oechel, W., Kobayashi, H., Humphreys, E., Goeckede, M., Iwata, H., Lafleur, P.M., Luoto, M., 2021. Statistical upscaling of ecosystem CO_2 fluxes across the terrestrial tundra and boreal domain: Regional patterns and uncertainties. Glob. Change Biol. 27 (17), 4040–4059. https://doi.org/10.1111/gcb.15659.

Wild, J., Kopecký, M., Macek, M., Šanda, M., Jankovec, J., Haase, T., 2019. Climate at ecologically relevant scales: a new temperature and soil moisture logger for long-term microclimate measurement. Agric. For. Meteorol. 268, 40–47. https://doi.org/10.1016/j.agrformet.2018.12.018.

Yang, Z., Hanna, E., Callaghan, T.V., Jonasson, C., 2012. How can meteorological observations and microclimate simulations improve understanding of 1913–2010 climate change around Abisko, Swedish Lapland? Meteorol. Appl. 19 (4), 454–463. https://doi.org/10.1002/met.276.

Zellweger, F., De Frenne, P., Lenoir, J., Rocchini, D., Coomes, D., 2019. Advances in microclimate ecology arising from remote sensing. Trends Ecol. Evol. 34 (4), 327–341. https://doi.org/10.1016/j.tree.2018.12.012.

Zellweger, F., De Frenne, P., Lenoir, J., Vangansbeke, P., Verheyen, K., Bernhardt-Römermann, M., Baeten, L., Hédl, R., Berkl, I., Brunet, J., van Calster, H., Chudomelová, M., Decocq, G., Dirnböck, T., Durak, T., Heinken, T., Jaroszewicz, B., Kopecký, M., Máliš, F., Coomes, D., 2020. Forest microclimate dynamics drive plant responses to warming. Science 368 (6492), 772–775. https://doi.org/10.1126/science.aba6880.